

EO-ALERT: A Novel Architecture for the Next Generation of Earth Observation Satellites Supporting Rapid Civil Alerts

*Original*

EO-ALERT: A Novel Architecture for the Next Generation of Earth Observation Satellites Supporting Rapid Civil Alerts / Kerr, M.; Tonetti, S.; Cornara, S.; Bravo, J. I.; Hinz, R.; Latorre, A.; Membibre, F.; Ramos, A.; Solimini, C.; Wiehle, S.; Breit, H.; Günzel, D.; Mandapati, S.; Tings, B.; Balss, U.; Koudelka, O.; Teschl, F.; Magli, E.; Bianchi, T.; Migliorati, A.; Motto Ros, P.; Caon, M.; Martina, M.; Freddi, R.; Milani, F.; Curci, G.; Fraile, S.; Marcos, C.. - ELETTRONICO. - (2021), pp. 1-8. (Intervento presentato al convegno 13th IAA SYMPOSIUM ON SMALL SATELLITES FOR EARTH OBSERVATION tenutosi a BERLIN, GERMANY (Virtual event) nel 27-29 APRIL 2021).

*Availability:*

This version is available at: 11583/2938192 since: 2021-11-18T14:28:12Z

*Publisher:*

IAA

*Published*

DOI:

*Terms of use:*

This article is made available under terms and conditions as specified in the corresponding bibliographic description in the repository

*Publisher copyright*

(Article begins on next page)

# EO-ALERT: A Novel Architecture for the Next Generation of Earth Observation Satellites Supporting Rapid Civil Alerts

M. Kerr<sup>1</sup>, S. Tonetti<sup>1</sup>, S. Cornara<sup>1</sup>, J. I. Bravo<sup>1</sup>, R. Hinz<sup>1</sup>, A. Latorre<sup>1</sup>, F. Membibre<sup>1</sup>, A. Ramos<sup>1</sup>, C. Solimini<sup>1</sup>, S. Wiehle<sup>2</sup>, H. Breit<sup>2</sup>, D. Günzel<sup>2</sup>, S. Mandapati<sup>2</sup>, B. Tings<sup>2</sup>, U. Balss<sup>2</sup>, O. Koudelka<sup>3</sup>, F. Teschl<sup>3</sup>, E. Magli<sup>4</sup>, T. Bianchi<sup>4</sup>, A. Migliorati<sup>4</sup>, P. Motto Ros<sup>4</sup>, M. Caon<sup>4</sup>, M. Martina<sup>4</sup>, R. Freddi<sup>5</sup>, F. Milani<sup>5</sup>, G. Curci<sup>5</sup>, S. Fraile<sup>6</sup>, C. Marcos<sup>7</sup>

<sup>1</sup>DEIMOS Space S.L.U.

Tres Cantos – Madrid, Spain

Email: {murray.kerr, stefania.tonetti, stefania.cornara, juan-ignacio.bravo, robert.hinz, antonio.latorre, francisco.membibre, alexis.ramos, chiara.solimini}@deimos-space.com

<sup>2</sup>Deutsches Zentrum für Luft- und Raumfahrt e.V.

Germany

Email: {stefan.wiehle, helko.breit, dominik.guenzel, srikantha.mandapati, bjoern.tings, ulrich.balss}@dlr.de

<sup>3</sup>Technische Universität Graz

Graz, Austria

Email: koudelka@tugraz.at, franz.teschl@tugraz.at

<sup>4</sup>Politecnico di Torino

Turin, Italy

Email: {enrico.magli, tiziano.bianchi, andrea.migliorati, paolo.mottoros, michele.caon, maurizio.martina}@polito.it

<sup>5</sup>OHB Italia Spa

Milan, Italy

Email: {riccardo.freddi, fabio.milani.ext, guido.curci.ext}@ohb-italia.it

<sup>6</sup>Deimos Imaging S.L.U.

Spain

Email: silvia.fraile@deimos-imaging.com

<sup>7</sup>Agencia Estatal de Meteorología

Madrid, Spain

Email: cmarcosm@aemet.es

**Abstract:** The EO-ALERT project proposes the definition and development of the next-generation Earth Observation (EO) data processing chain, based on a novel flight segment architecture that moves optimised key EO data processing elements from the ground segment to on-board the satellite, with the aim of delivering EO products to the end user with very low latency. EO-ALERT achieves, globally, latencies below five minutes for EO products delivery, and below 1 minute in some scenarios. The proposed architecture combines innovations in the on-board elements of the data chain and the communications, namely: on-board reconfigurable data handling, on-board image generation and processing for the generation of alerts (EO products) using Artificial Intelligence (AI), on-board AI-based data compression and encryption, high-speed on-board avionics, and reconfigurable high data rate communication links to ground, including a separate chain for alerts with minimum latency and global coverage. This paper presents the proposed architecture, its performance and hardware, considering two different user scenarios: ship detection and extreme weather nowcasting. The results show that, when implemented using COTS components and available communication links, the proposed architecture can deliver alerts to ground with latency below five minutes, for both SAR and Optical missions, demonstrating the viability of the EO-ALERT concept.

# 1. INTRODUCTION

The classical Earth Observation (EO) data chain generates a severe bottleneck, given the very large amount of raw data generated on-board the satellite that must be transferred to ground, slowing down the EO product availability, increasing latency, and hampering applications to grow in accordance with the increased user demand for EO products. This paper provides an overview of the **EO-ALERT project** (<http://eo-alert-h2020.eu/>), an H2020 European Union research activity that proposes the definition and development of the **next-generation EO data and processing chain**, based on a novel flight segment architecture that moves optimised key EO data processing elements from the ground segment to on-board (O/B) the satellite. The objective is to deliver the EO products to the end user with very low latency and increased throughput [17]. Achieving this goal requires **innovation in several critical technological areas**: O/B reconfigurable data handling, O/B image generation and processing, high-speed O/B avionics, O/B data compression and reconfigurable high data rate communication links to ground.

# 2. EO-ALERT OVERVIEW

Data latency has become a key requirement in the EO market, since end-users require that data is available in very short time intervals in the order of 30 to 15 min. Data latency can be defined as the interval from the data collection to the time when the data is converted to a specified EO product and delivered to the users. Based on this definition, EO-ALERT has a **goal latency of less than 1 min** and requires a maximum latency below 5 min for both Synthetic Aperture Radar (SAR) and optical image products. With modern more powerful computational systems, it is conceivable to generate data products directly on-board, reducing the time needed from hours to a few minutes (Figure 1).

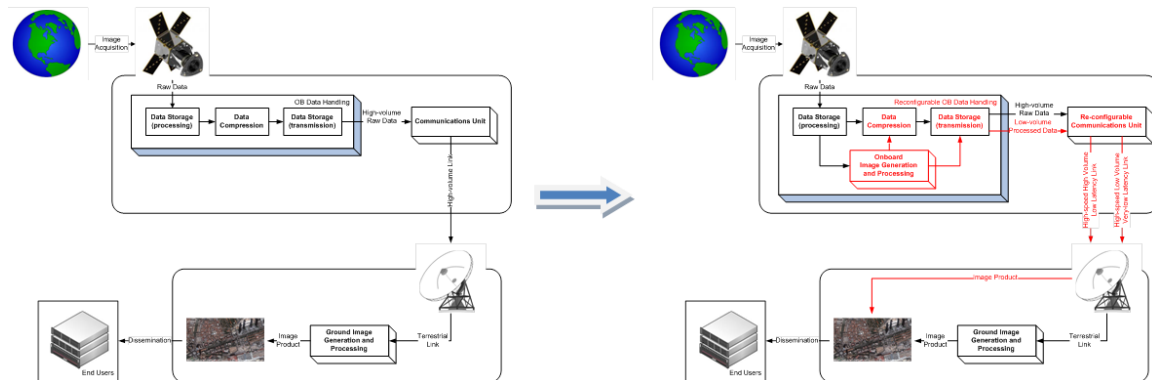


Figure 1: EO-ALERT data chain: (left) classical data chain based on raw data compression and transfer, (right) innovative data chain showing its key elements and new data flows (in red)

The proposed novel satellite processing chain has implications on several technological areas, including high-speed avionics, Flight Segment/Ground Segment (FS/GS) communications, O/B compression and data handling and O/B image generation and processing. The project develops both the technologies and the data handling architecture, with an approach aimed at optimising the use of O/B resources, as well as making the most out of the available image data through direct O/B processing. Recently developed image compression concepts aimed at improving image quality for a given compression ratio, while maximizing throughput, will be adopted for the first time in space applications. Both the technologies and their integrated chain are **verified and experimentally evaluated** on an avionics test-bench, using first relevant EO historical sensor data, and

then demonstrated through relevant end-to-end tests, in which EO data acquired specifically for EO-ALERT are injected in the system and results are obtained, evaluated and benchmarked. Ground truth data for evaluation has been obtained through an experimentation campaign on a real and representative test-field, successfully run in July 2020. Namely, EO-ALERT identified two main scenarios for testing the potential of the proposed high-speed data chain: **ship detection** and **extreme weather monitoring**.

The most common needs of maritime users [15] encompass small ground resolution ( $\leq 1\text{m}$ ), low revisit time ( $\leq 6$  hours between consecutive observations), flexibility (to choose the image acquisition date) and responsiveness (to make last-minute changes to the image request). SAR satellites are the most suitable for ship detection, whereas very high-resolution (HR) optical imagery reduces false positives and allows ship identification. For the EO-ALERT project, Deimos-2 and TerraSAR-X have been selected for the optical imagery and radar data. Multiple tests are proposed with the objective to send a **maritime alert**, similar to the EMSA Vessel Detection Service, to an end user including position information, movement information, image clipping data and ship details with a very short latency ( $\leq 5$  min), and the bulk data (raw data, etc.) later with a more relaxed latency ( $\leq 30$  min).

The EO-ALERT technology can be very beneficial for the generation of meteorological products with high quality and low latency. In the **Extreme Weather Scenario** [16], **convective storms** are detected in all the convection stages using Geostationary (GEO) satellite data, focusing on their monitoring and providing information on storm location, trajectory and characteristics. A 4-step algorithm consisting of candidate cell extraction, tracking, convective stage discrimination and alert generation, is being developed. OPERA [8] radar network data is being used as ground truth. Qualitative comparison of the EO-ALERT algorithm with the operational NWCSAF [9] RDT-CW (Rapidly Developing Thunderstorms - Convection Warning) shows compatible results for the cell extraction and convective discrimination. The EO-ALERT satellite-derived sea surface information on wind speed and wave height can enable more accurate models of storm field trail and development on the open sea, allowing to circumvent a storm.

### 3. EO-ALERT ARCHITECTURE

#### 3.1 Functional and Physical Architecture

The proposed architecture is designed to be modular, scalable and reconfigurable, so as to be suitable for several scenarios. The entire data-chain is divided into several functional blocks, each one implemented on dedicated software and/or hardware computing resources. With this approach, the system can process different data types (e.g. optical and SAR data) from several sensors over a wide range of dataset sizes. The top-level architecture of the EO-ALERT system can be divided into three main physical blocks. The **Sensor Board** acquires raw image data from the sensor(s) and transfers it to the Processing Board using an acquisition memory buffer. The **Processing Board** consists of several Multi-Processor System-on-Chip (MPSoC) devices that integrate a multi-core Processing System (PS) and a Programmable Logic (PL) part. The Processing Board fetches the raw data from the acquisition buffer and implements all the data processing tasks required to yield the EO products (e.g. alerts and generated images): 1) Optical image generation and processing, 2) SAR image generation and processing, 3) Central Processing Unit (CPU) Scheduling, Compression/Encryption and Data Handling (CS-CEDH). Computationally expensive tasks, such as image processing or image compres-

sion/encryption, are partially or completely implemented in hardware. Depending on the workload, one or more MPSoC devices may be assigned to the same task. Less demanding tasks (execution flow control, data routing, simple data processing) are performed by the software running on the PS CPU cores of each device. The **TX/RX Subsystem** receives data (EO products, alerts, raw data, ancillary data) from the Processing Board, and forwards it to the ground segment using either a very-low latency channel for critical data (i.e. alerts) or a high data rate channel for large data (e.g. generated images).

The Avionics physical design is implemented as a hybrid solution that uses both Commercial Off-The-Shelf (COTS) and space-qualified components [6] [7]. COTS are used in conjunction with mitigation techniques to increase robustness of the design against radiation effects, whereas space-qualified components are used for the critical functions. This choice allows keeping weight, volume and cost of the **Payload Data Processing Unit (PDPU)** low with respect to an all space-grade design and it takes advantage of the state-of-the-art technology and processing power of the latest COTS components. All boards are based on the powerful Xilinx Zynq US+ ZU19EG MPSoC featuring a quad core ARM processor and a large Field-Programmable Gate Array (FPGA) built onto the same die so that processing algorithms can benefit from hardware acceleration.

### 3.2 Optical Image Generation and Processing

The **O/B Optical Image Generation** provides a HR image product for latency-driven scenarios and enables the **Image Processing** stage by generating a denoised and artifact-free image. The O/B L1 product consists of: 1) HR calibrated and denoised image, 2) geolocation information, 3) HR sea-land binary mask (3m/pixel). The raw data obtained from the payload is calibrated to remove pixel inconsistencies and to convert the pixel digital counts to radiances. The calibrated image is processed with an edge-aware denoising algorithm based on optimised convolutional operations. The position provided by the satellite GPS and the attitude provided by the AOCS are used to geolocate the image corners. The geolocation algorithm is prepared to integrate Earth Orientation Parameters that can be sent to the spacecraft (S/C). The geolocation information is used to retrieve the sea-land pixel binary mask that is stored on-board. To avoid decompressing the whole land-mask on-board, which could lead to memory issues, the minimum chunk of information required to generate the sea-land mask for the image is extracted and decompressed on the O/B memory. The sea-land mask is projected onto the image coordinates to assign sea-land information to the image pixels.

The **ship detection algorithm** is applied to HR panchromatic images and consists of a 3-step approach: 1) candidate ship extraction, 2) AI-based ship discrimination, 3) fusion. The first step provides regions of the image that have ship-alike shapes and intensities, using Otsu thresholding [12] combined with intensity and shape metrics. This information is fused with the land-sea mask to remove areas detected over land regions. In the ship discrimination step, each image region from the binary image is labelled independently using the algorithm from [13]. The regions from the image, corresponding to the labels from the binary image, are described using feature representations and classified with Machine Learning (AI-based) classifiers to assess the presence of a ship. The last step, fusion, removes ships detected on overlapping areas of the image (if the image is divided over different boards) or to suppress different detections of the same object.

In the **extreme weather scenario**, convective storms are detected from GEO S/C images using a 3-step algorithm: 1) candidate cell extraction, 2) candidate cell tracking, 3) AI-based convective cell discrimination. Candidate convective cells are detected as lo-

cal temperature minima in brightness temperature images derived from GEO S/C data. Cell position and velocity are tracked over time by matching candidate cells between images of subsequent acquisitions based on spatial overlap in the corresponding maps. Ambiguities in the assignment due to cell merging or splitting are filtered to produce unique tracks. A machine learning classifier, trained on ground truth data generated from composites of Meteosat-SEVIRI images and OPERA weather radar network data, performs convective cell discrimination. Each cell is characterized by its brightness temperatures in 5 infrared channels in SEVIRI imagery and their evolution over time.

### 3.3 SAR Image Generation and Processing

Precise HR SAR image generation from satellite raw data is a complex and computationally expensive task. Considering TerraSAR-X as space segment, a full adaptation of the existing focusing processor, which uses the Chirp Scaling algorithm [5], is not foreseen. Based on the EO-ALERT objectives, the wave number domain Omega-K ( $\omega$ KA) algorithm [1] (“monochromatic  $\omega$ KA” approximate version) is selected to enable SAR image formation with resolution below 3m. **SAR image generation** covers signal processing of the sensor data and computation of processing and annotation parameters. Signal processing, such as raw data correction, Fast Fourier Transform/Inverse Fast Fourier Transform, antenna pattern correction, detection and multi-looking, demands high computation power, resources and input/output throughput; so this part of the algorithm is implemented in the MPSoC PL with parallelization. Processing and annotation parameters, such as geometric doppler centroid determination, SAR focusing parameter and geolocation, are calculated on the MPSoC PS ARM cores as a software.

The **ship detection algorithm** [2] involves three image processing steps: 1) initial detection, 2) refinement, 3) filtering. A Constant False Alarm Rate algorithm is used in the first step. Each pixel intensity has to be compared to the mean intensity of its surrounding area: this step is computationally very expensive and it is implemented in hardware. The refinement step investigates the surrounding of all ship candidates to find additional ships close-by which were missed in the initial detection. Filtering removes azimuth ambiguities created during the image processing and applies land masking to remove all detections on land. Detections left after this step are considered detected ships and their properties (e.g. location, dimensions, heading) are gathered.

For the **extreme weather scenario**, the ocean surface wind speed and wave height are derived from the SAR image processing in three steps: 1) image tiling, 2) wind speed detection, 3) sea state detection. The image is divided into a grid of sub-scenes of configurable size, and wind and sea state detection is performed on each individual sub-scene. Wind speed detection employs the Geophysical Model Function XMOD2 [3] previously tuned on TerraSAR-X archived images, calculating wind speed from sea surface backscatter. For sea state detection, the empirical XWAVE algorithm [4] is used. The resulting product includes wind speed and wave height on a per-sub-scene basis.

### 3.4 CPU Scheduling, Compression, Encryption & Data Handling (CS-CEDH)

The following operations are performed by the software running on the CPU in the PS of one of the MPSoC devices, except for image compression and encryption that is implemented in hardware on the PL to increase compression and encryption throughput.

- Acquire raw data from the Sensor Board and ancillary data from the O/B ancillary data source, and forward the raw, ancillary and configuration data to the target optical or SAR Image Processing modules.

- Acquire EO products (e.g. alerts, generated images, etc.) from the Image Processing modules once they are ready, and compress and/or encrypt the raw data, ancillary data and EO products.
- Store compressed/encrypted data on the O/B storage, and send them to the TX/RX Subsystem for transmission to the ground segment.

**Compression of optical and SAR raw sensor data and generated images** is achieved using a hardware implementation of a method based on the CCSDS 123.0-B-2 standard [10]. The compression algorithm has been extended to embed image encryption by sign-randomization of the prediction residuals [11]. A flexible and reconfigurable digital core has been designed so that it is not tied to a specific FPGA family, eventually targeting different timing constraints, resource utilization and performance. Performance tests on the target platform, on real-case test images and with timing measurements, showed that about 10s are required to compress and encrypt an optical 10000x10000 image. The software running on the PS splits each image into multiple sub-sets of along-track lines (tiling), and each sub-set is compressed and encrypted individually by the hardware IP core. This allows most of the image to be successfully reconstructed even when some data is lost while delivering the image to the ground segment. Tiling also enables parallel image compression and encryption on multiple IP cores if the target platform features enough hardware resources. The software running on the CS-CEDH MPSoC PS CPU schedules **data transfers to the TX/RX Subsystem**, allocating “high” priority to alerts and “low” priority to other data. Each transmission unit (compressed/encrypted file or sub-file from a tiled image) is split into a stream of CCSDS packets sent to the TX/RX Subsystem over a high-speed communication channel with 1Gbit/s throughput on the target platform. Considering the packetization overhead and the storage read performance, the largest transmission unit is transferred in less than 100ms (maximum delay between alert encryption and its transfer to the TX/RX subsystem).

### 3.5 Communications

The communications system delivers EO products, bulk (raw and generated image) data and alerts (O/B processed and generated) locally and globally at high speed with minimum latency. The latency requirement is 5 min for alerts for both local and global delivery, and 30 min for raw data/images for global delivery.

The first high-speed data payload operates in Ka-band (25.5–27 GHz), which is assigned for EO and provides more bandwidth than X-band. The transmitter consists of a modem/codec (supporting QPSK, 8PSK, 16APSK and 64APSK modulation schemes) and an upconverter unit. 10W Ka-band solid-state power amplifier amplifies the signal and delivers it to a 25dBi-gain horn antenna. The system is fully redundant and supports data rates up to 2.6 Gbit/s.

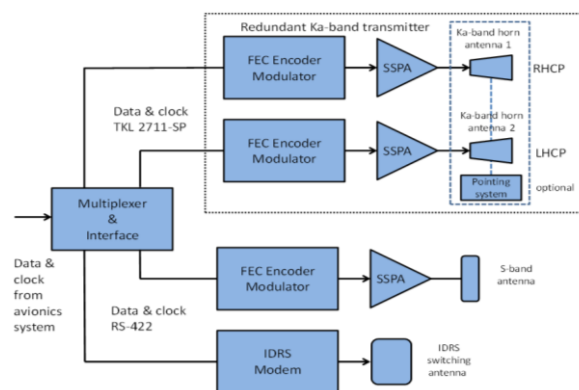


Figure 2: Communications System Block Diagram

The Ka-band system is used for both **bulk data and alerts to local ground stations**. The second payload consists of an S-band transmitter for alerts only, supporting data rates up to 1 Mbit/s to small and inexpensive hand-held terminals for rescue teams.

Bulk data can be delivered globally within 30 min via Ka-band, if a network of at least 13 ground stations around the globe is used. An alternative global broadband solution is the use of an optical terminal on board of the EO spacecraft and a data relay service such as the European Data Relay Satellite System (EDRS). Another solution for **global delivery of alerts** consists in using the INMARSAT satellite network and a compact product for the O/B transceiver provided by the company ADDVALUE [14] (iDRS service). The iDRS service is envisaged for the short-term EO-ALERT solution providing a data rate of 250 kbit/s. About 100 alerts can be transferred in 37 seconds.

#### 4. HIGH-SPEED AVIONICS TEST-BENCH AND RESULTS

The Avionics Test-Bench (TB) consists of a scaled-down version of the Avionics Subsystem, offering four boards instead of seven. To resemble the PDPU as much as possible, one board is dedicated CS-CEDH while the other three are dedicated to processing. TB boards are also interconnected, so that the complete data chain is reproduced and a realistic latency measurement can be obtained. A standard Gigabit Ethernet connection connects the TB to a TX/RX subsystem emulator to test the transmission to Ground Segment. The TB can be configured to process OPT or SAR data using an external PC and dedicated Ethernet links to each board. To inject real OPT and SAR data in the TB, raw images are loaded into a SSD connected to the CS-CEDH board, providing inputs that should come from sensors in the final system.

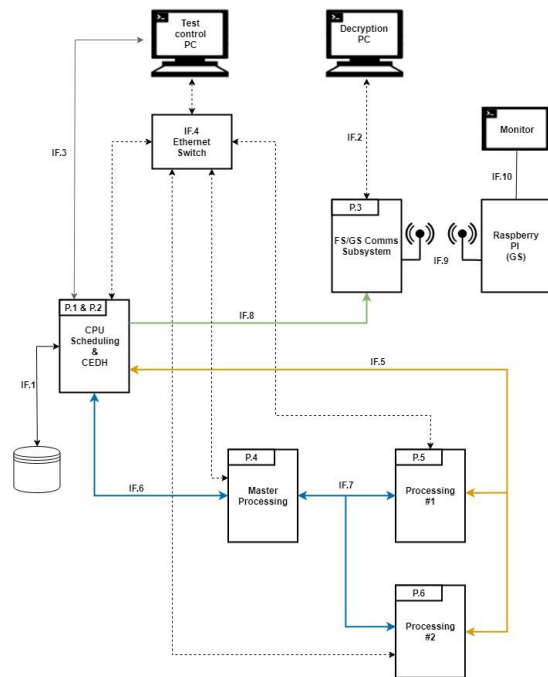


Figure 3: Test-Bench Architecture

For the **ship scenario** the **optical processing** is performed in a configurable multi-board scheme. Each board processes 2 raw data blocks of about  $8000 \times 6000$  points covering about  $9\text{km} \times 6\text{km}$  ( $54 \text{ km}^2$ ) each, i.e.  $\sim 100 \text{ km}^2$  per board. To process this area, the **entire processing chain takes 35 s running on a single board**. In a multi-board scheme where it is possible to process  $300 \text{ km}^2$  in parallel,  $900 \text{ km}^2$  can be processed in  $\sim 110 \text{ s}$  and  $1200 \text{ km}^2$  in  $\sim 150 \text{ s}$ , assuming transfer delays and management tasks. For the **weather scenario** data is processed in a dual-board scheme with only one processing board. The processed images have about  $1200 \times 650$  pixels with  $3 \text{ km/pixel}$  of GSD, covering almost  $7 \cdot 10^6 \text{ km}^2$ . Assuming transfer delays and management tasks, it is possible to have the **products ready in about 15 s**.

The **SAR processing** is run on a single board. The sensor input consists of 1-3 raw data blocks of  $8192 \times 32768$  points each, covering an area of  $12.5 \text{ km} \times 30 \text{ km}$  per block. The image generation for one block takes 4 s, and image processing takes 30 s for the ship scenario and 35 s for the extreme weather scenario using a raster size of  $2 \text{ km} \times 2 \text{ km}$ . Hence, the **SAR processing total runtime for a single block is below 40 s**. Multiple blocks are calculated successively, hence, the total runtime for three is below 120 s.



## 5. CONCLUSIONS & WAY FORWARD

This paper provides an overview of the EO-ALERT project objectives, innovations and results. Results obtained from current hardware testing show that the demanding objective of providing EO products with latency below 5 min can be achieved and **global EO product latencies below 1 min** are obtained in realistic scenarios. The architecture is targeted to the generation of alerts in the ship detection and extreme weather monitoring scenarios; however, it is quite general and can be easily adapted to alternative scenarios. The proposed architecture can be efficiently implemented relying on a combination of space-qualified components and high-performance COTS components. The EO-ALERT project will run until end of 2021 and the remaining activities cover the full data chain integration and the verification into the avionics test bench. Overall results of the entire project, including the experimental campaign and validation of the avionics test bench, will be presented to end-users and possible commercial partners during the final EO-ALERT workshop.

## 6. REFERENCES

- [1] Bamler, R (1992) A Comparison of Range-Doppler and Wavenumber Domain SAR Focusing Algorithms, *IEEE Trans. On Geoscience and Remote Sensing*, 30 (4), 706-713
- [2] Tings, B. & al. (2016) Dynamically adapted ship parameter estimation using TerraSAR-X images, *Int J Remote Sens*, 37:9, 1990-2015, DOI: 10.1080/01431161.2015.1071898
- [3] Li, X.-M., Lehner, S. (2014) Algorithm for sea surface wind retrieval from TerraSAR-X and TanDEM-X data, *IEEE Trans Geosci Remote Sens.*, 52, 5, 2930-2941
- [4] Pleskachevsky, A.L. & al. (2016) Meteo-Marine Parameters for Highly Variable Environment in Coastal Regions from Satellite Radar Images. *ISPRS J. Photogr. Remote Sens.*, 119, 464-484
- [5] Raney, R.K. & al. (1994) "Precision SAR Processing Using Chirp Scaling," *IEEE Transactions on Geoscience and Remote Sensing (TGRS)*, Vol. 32, pp. 786-799
- [6] D. Sinclair, J. Dyer, "Radiation effects and COTS parts in SmallSats", in *Conference on Small Satellites, SSC13-IV-3K*, 2013
- [7] A. LaBel, "Commercial Off The Shelf (COTS): Radiation Effects Considerations and Approaches", in *NEPP Electronic Technology Workshop*, 2012
- [8] <http://eumetnet.eu/activities/observations-programme/current-activities/opera/>, last retrieved 18/09/2020
- [9] <http://www.nwcsaf.org/>, last retrieved 18/09/2020
- [10] Consultative Committee for Space Data Systems (CCSDS), "Low-Complexity Lossless and Near-Lossless Multispectral and Hyperspectral Image Compression," *Blue Book*, no. 1, February 2019
- [11] A. Migliorati & al., "Selective encryption in the CCSDS standard for lossless and near-lossless multispectral and hyperspectral image compression", *Proceedings Volume 11533, Image and Signal Processing for Remote Sensing XXVI*; 1153312 (2020)
- [12] Otsu, N. (1979). A threshold selection method from gray-level histograms. *IEEE transactions on systems, man, and cybernetics*, 9(1), 62-66
- [13] Wu, K. & al. (2009). Optimizing two-pass connected-component labeling algorithms. *Pattern Analysis and Applications*, 12(2), 117-135
- [14] <https://www.addvaluetech.com/inter-satellite-data-relay-system-idrs/>
- [15] S. Tonetti & al., "EO-ALERT: Next Generation Satellite Processing Chain for Security-Driven Early Warning Capacity in Maritime Surveillance and Extreme Weather Events", 2019 Living Planet Symposium, 13-17 May 2019, MiCo - Milano Congressi, Milan, Italy
- [16] A. Fiengo & al., "EO-ALERT - Extreme Weather Scenario: Towards Convective Storm Nowcasting via On-Board Satellite Processing", 3<sup>rd</sup> European Nowcasting Conference, 24-26 April 2019, Madrid
- [17] Kerr M. & al., "EO-ALERT: A Novel Flight Segment Architecture for EO Satellites Providing Very Low Latency Data Products", *ESA Phi-week 2019*, 9-13 Sep., ESA-ESRIN, Frascati, Rome